Determination of the beam asymmetry Σ in η- and η'-photoproduction using Bayesian statistics

Jakob Michael Krause

Masterarbeit in Physik
angefertigt im Helmholtz-Institut für Strahlen- und Kernphysik

vorgelegt der
Mathematisch-Naturwissenschaftlichen Fakultät
der
Rheinischen Friedrich-Wilhelms-Universität
Bonn

Sep 2022

I hereby declare that this thesis was formulated by myself and that no sources or tools other than those cited were used.

Bonn, ...
Date   Signature

1. Gutachterin: Jun. Prof. Dr. Annika Thiel
2. Gutachter: Prof. Dr. Jochen Dingfelder

Contents

CHAPTER 4

Extraction of the beam asymmetries Σ_η and $\Sigma_{\eta'}$

The beam asymmetry Σ is observable when a linearly polarized photon beam and unpolarized liquid hydrogen target are employed. The polarized cross section $\frac{d\sigma}{d\Omega}_{pol}$ is not symmetric in the azimuthal angle ϕ anymore as opposed to the unpolarized cross section $\frac{d\sigma}{d\Omega}_0$. It is rather modulated by a cosine dependence which scales with the polarization observable Σ and the (linear) beam polarization p_γ, see equation (4.1) [San+11].

$$\frac{d\sigma}{d\Omega}_{pol}\left(E_\gamma, \cos\theta, \phi\right) = \frac{d\sigma}{d\Omega}_0\left(E_\gamma, \cos\theta\right) \cdot \left[1 - p_\gamma \Sigma\left(E_\gamma, \cos\theta\right)\cos\left(2\varphi\right)\right] \tag{4.1}$$

Since the incident photon beam is polarized, photon momentum $\vec{k}$ and polarization $\vec{\epsilon}$ span a plane which is referred to as the beam polarization plane. This plane is tilted by the angle φ with respect to the reaction plane which is defined by the final state momenta. Naturally, this plane builds the angle ϕ in the laboratory system. At the same time the angle of the beam polarization plane in the same reference frame is defined as α. It holds

$$\varphi = \alpha - \phi. \tag{4.2}$$

Figure 4.1 illustrates definitions of all angles and planes. Theoretically the beam asymmetry can be

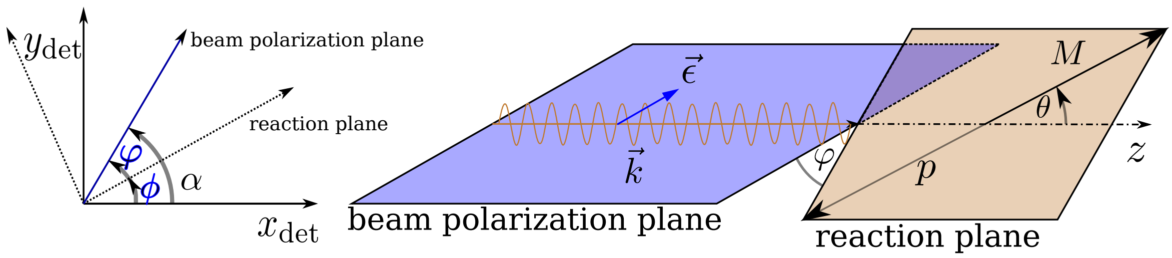

Figure 4.1: Left: Definition of angles α, ϕ, φ. Right: Photon momentum $\vec{k}$ and polarization $\vec{\epsilon}$ define the beam polarization plane while the reaction plane is defined by the recoil proton p and produced meson M.

determined by a measurement of the cross section and a fit using equation (4.1). However, when calculating polarized cross sections, it is important to have good control over flux normalization and detector acceptance in three dimensions $(E_\gamma, \cos\theta, \phi)$. To avoid this, the measurement of asymmetries can be used to access the polarization observable Σ instead. Particularly, data is taken for two distinct orthogonal polarization settings corresponding to $\alpha = \pm 45^\circ$.

This chapter will illustrate the process of determining the beam asymmetry for η and η' photoproduction. The published results of Σ_η [Afz19; Afz+20] are used to check the accuracy and functionality of employed bayesian methods. Bayesian methods, as well as traditional frequentist approaches are used afterwards to extract new results for $\Sigma_{\eta'}$. First, the used methods will be presented and subsequently their application for each final state, respectively.

4.1 Methods

The beam asymmetry has to be determined via fits to ϕ distributions obtained from data. These are performed as either binned or unbinned fits. Both methods allow the application of Bayesian methods as will be discussed in the following. Additionally the advantages and disadvantages off all methods are compared.

4.1.1 Event yield asymmetries

Measurements were made in two distinct polarization settings $\alpha = \pm 45^\circ = \alpha^{\perp/\parallel}$. Thus, the polarized cross sections for both settings are given by[1]

$$\frac{\mathrm{d}\sigma}{\mathrm{d}\Omega}^{\parallel}_{\mathrm{pol}} = \frac{\mathrm{d}\sigma}{\mathrm{d}\Omega}_{0} \cdot \left[1 - p_\gamma^{\parallel}\Sigma\cos\left(2\left(\alpha^{\parallel} - \phi\right)\right)\right] \tag{4.3}$$

and

$$\frac{\mathrm{d}\sigma}{\mathrm{d}\Omega}^{\perp}_{\mathrm{pol}} = \frac{\mathrm{d}\sigma}{\mathrm{d}\Omega}_{0} \cdot \left[1 - p_\gamma^{\perp}\Sigma\cos\left(2\left(\alpha^{\perp} - \phi\right)\right)\right] \tag{4.4}$$

$$= \frac{\mathrm{d}\sigma}{\mathrm{d}\Omega}_{0} \cdot \left[1 + p_\gamma^{\perp}\Sigma\cos\left(2\left(\alpha^{\parallel} - \phi\right)\right)\right]. \tag{4.5}$$

Note that equation (4.5) holds, because

$$\alpha^{\perp} = \alpha^{\parallel} + \pi/2 \qquad \text{and} \qquad \cos x = -1 \cdot \cos(x + \pi).$$

Consider now taking the difference of equations (4.3) and (4.5)

$$\frac{\mathrm{d}\sigma}{\mathrm{d}\Omega}^{\perp}_{\mathrm{pol}} - \frac{\mathrm{d}\sigma}{\mathrm{d}\Omega}^{\parallel}_{\mathrm{pol}} = \frac{\mathrm{d}\sigma}{\mathrm{d}\Omega}_{0} \cdot \left(p_\gamma^{\perp} + p_\gamma^{\parallel}\right)\Sigma\cos\left(2\left(\alpha^{\parallel} - \phi\right)\right). \tag{4.6}$$

One can further eliminate the unpolarized cross section from this equation by dividing by the polarization weighted sum of equations (4.3) and (4.5)

$$\alpha \cdot \frac{\mathrm{d}\sigma}{\mathrm{d}\Omega}^{\parallel}_{\mathrm{pol}} + \beta \cdot \frac{\mathrm{d}\sigma}{\mathrm{d}\Omega}^{\perp}_{\mathrm{pol}} = \frac{\mathrm{d}\sigma}{\mathrm{d}\Omega}_{0} \cdot \left[\alpha + \beta - \left(\alpha p_\gamma^{\parallel} - \beta p_\gamma^{\perp}\right)\Sigma\cos\left(2\left(\alpha^{\perp} - \phi\right)\right)\right] \stackrel{!}{=} 2\frac{\mathrm{d}\sigma}{\mathrm{d}\Omega}_{0}. \tag{4.7}$$

[1] The dependencies of polarized and unpolarized cross sections as well as the beam asymmetry like in equation (4.1) are implied

Since

$$\frac{\mathrm{d}}{\mathrm{d}\phi}\frac{\mathrm{d}\sigma}{\mathrm{d}\Omega}_0 \stackrel{!}{=} 0 \forall \phi,$$

it holds

$$\alpha p_\gamma^\parallel - \beta p_\gamma^\perp \stackrel{!}{=} 0 \qquad\qquad \alpha + \beta \stackrel{!}{=} 2, \tag{4.8}$$

such that

$$\alpha = \frac{2p_\gamma^\parallel}{p_\gamma^\perp + p_\gamma^\parallel} \qquad\qquad \beta = \frac{2p_\gamma^\perp}{p_\gamma^\perp + p_\gamma^\parallel}. \tag{4.9}$$

The beam asymmetry Σ is thus accessible via the asymmetry

$$A(\phi) = \frac{\frac{\mathrm{d}\sigma}{\mathrm{d}\Omega}^\perp_{\mathrm{pol}} - \frac{\mathrm{d}\sigma}{\mathrm{d}\Omega}^\parallel_{\mathrm{pol}}}{p_\gamma^\parallel \frac{\mathrm{d}\sigma}{\mathrm{d}\Omega}^\perp_{\mathrm{pol}} + p_\gamma^\perp \frac{\mathrm{d}\sigma}{\mathrm{d}\Omega}^\parallel_{\mathrm{pol}}} = \Sigma \cos\left(2\left(\alpha^\parallel - \phi\right)\right). \tag{4.10}$$

At this point one can now make use of the fact that in any scattering reaction the number of events N is given by the product of luminosity L and total cross section σ

$$N = L \cdot \sigma = \Phi \cdot N_t \cdot \frac{\mathrm{d}\sigma}{\mathrm{d}\Omega} \cdot \Delta\Omega,$$

where Φ is the beam flux, N_t the number of target particles and $\Delta\Omega$ is the solid angle covered by the detector. Substituting this in equation (4.10) one can build the asymmetry $A(\phi)$ using only the (flux-)normalized event yields $\tilde{N}^{\parallel/\perp}\left(E_\gamma, \cos\theta, \phi\right)$[2]

$$A(\phi) = \frac{\tilde{N}^\perp - \tilde{N}^\parallel}{p_\gamma^\parallel \tilde{N}^\perp + p_\gamma^\perp \tilde{N}^\parallel} = \Sigma \cos\left(2\left(\alpha^\parallel - \phi\right)\right). \tag{4.11}$$

Alternatively, the event yields N can also be normalized by integrating over the total azimuthal angle range in each bin of $(E_\gamma, \cos\theta)$. This normalization technique has been used in reference [Afz19] and will also be used in this work. Using appropriate binning in ϕ in addition to beam energy and meson polar angle the asymmetry can be build for all kinematic bins and the beam asymmetry then be extracted via a one-Parameter fit. The statistical errors for $A(\phi)$ are given by Gaussian error propagation (see appendix A.1).

Frequentist

The beam asymmetry can now be determined via a frequentist fit, where Σ is determined such that the χ^2 value resulting from the data points and equation 4.11 is minimized. The results are point estimates with statistical error bars that are also obtained from the fit: $\hat{\Sigma} \pm \sigma_{\hat{\Sigma}}$. In addition $\chi^2/\mathrm{NDF} \approx 1$ may be verified in order to diagnose the fit itself. Multiple automated minimization and calculation algorithms

[2] again, arguments $\left(E_\gamma, \cos\theta, \phi\right)$ are implied.

for χ^2 fitting are available as open source. The *Python* [RP22] module *scipy* [Vir+20] and *ROOT* [BR97] offer e.g. the methods `scipy.optimize.curve_fit` [sci] and `TH1::Fit()` [ROOa] for discrete/binned data, which were used in the analysis.

Bayesian

Following section 1.3, where the basics of Bayesian inference were discussed, the goal of a Bayesian approach is to sample marginal posterior distributions for each fitted parameter from the joint posterior $p(\boldsymbol{\theta}|y)$ which depends on the observed data y. The joint posterior itself is proportional to the product of priors $\pi(\boldsymbol{\theta})$ and likelihood $\mathcal{L}(y|\boldsymbol{\theta})$ (Bayes' theorem). This collapses to a one parameter problem in the case of fitting the event yield asymmetries (Eq. (4.11))

$$p(\Sigma|y) \propto \pi(\Sigma) \cdot \mathcal{L}(y|\Sigma). \tag{4.12}$$

However, to be able to sample from a joint posterior, prior and likelihood need to be specified. In order not to bias the fit towards any particular values, the prior is chosen non-informative, realized by a broad Gaussian centered at 0 which is truncated to the physically allowed parameter space of $\Sigma \in [-1, 1]$. Furthermore, the likelihood is formulated assuming Gaussian errors ϵ_n at each data point y_n, which should be described by the asymmetry (Eq (4.11)) at bin n $A(\phi_n; \Sigma)$, i. e. [3]

$$\Sigma \sim \mathcal{N}(0,1)_{[-1,1]} \qquad y_n = A(\phi_n;\Sigma) + \epsilon_n \qquad \epsilon_n \sim \mathcal{N}(0, \sigma_n), \tag{4.13}$$

which is equivalent to

$$\Sigma \sim \mathcal{N}(0,1) \qquad y_n \sim \mathcal{N}\left(A(\phi_n;\Sigma), \sigma_n\right). \tag{4.14}$$

The likelihood of all data points now evaluates to the product of the likelihood at each data point y_n and the posterior results in

$$p(\Sigma|y) \propto \pi(\Sigma) \cdot \mathcal{L}(y|\Sigma) = \mathcal{N}(\Sigma|0,1)_{[-1,1]} \cdot \prod_n \mathcal{N}\left(y_n | A(\phi_n;\Sigma), \sigma_n\right) \tag{4.15}$$

$$\Leftrightarrow -\ln p(\Sigma|y) = \frac{1}{2}\Sigma^2 + \frac{1}{2}\sum_n \left(\frac{y_n - A(\phi_n;\Sigma)}{\sigma_n}\right)^2 + \text{ constant terms }, \tag{4.16}$$

such that all ingredients are present to form a fully Bayesian probabilistic model[4]. This model was implemented in Stan [Sta22], directly giving access to samples from the posterior obtained with the No-U-Turn-Sampler (NUTS) [Sta22; HG14]. Hereby, the sampling is restricted to the allowed parameter region $\Sigma \in [-1, 1]$. As a measure of goodness of fit, the p-values obtained from the posterior predictive distributions, as introduced in section 1.3, are reviewed. To diagnose the convergence of the MCMC fit, sensible values for $\hat{R}$ and the Monte-Carlo standard error σ_{MCSE} are verified.

[3] Remember the notation introduced in section 1.3: $x \sim \mathcal{N}(\mu,\sigma) = \mathcal{N}(x|\mu,\sigma) = \frac{1}{\sqrt{2\pi\sigma^2}} e^{-\frac{(x-\mu)^2}{2\sigma^2}}$

[4] Note that the sampling aims only to reflect the right proportionality of the (marginal) posterior. Thus, constant terms can be dropped and are of no further interest [Sta22].

4.1.2 Event based fit

Although intuitive and easily implementable the binned fit –Bayesian or not– has one critical disadvantage: it is inevitable that information is lost because the asymmetry $A(\phi)$ is a binned quantity and hence, the choice of binning influences the fit results. This will be discussed in more detail in section 4.1.3. Especially kinematic bins with low statistics show this behavior. To circumvent this problem, an *unbinned fit*, based on the likelihood function for each event, can be performed. Also, no assumptions on the distribution of statistical errors have to be made since each event is taken into account individually. Yet, the event based fit does not provide any measure of goodness of fit, so that the study of toy Monte Carlo data is essential when checking the working principle of the method.

In a polarized experiment the azimuthal angle distribution of events is not isotropic, but modulated by a cosine term coupling to beam asymmetry Σ and beam polarization $p_\gamma^{\parallel/\perp}$ for each setting $\alpha^{\parallel/\perp}$, as is expressed through the respective differential cross sections in Equations 4.3 and 4.4. Since the number of events is proportional to the cross section, the probability $p\left(\phi, p_\gamma^{\parallel/\perp}|\Sigma\right)$ to find an event under the azimuthal angle ϕ for a given bin of $\left(E_\gamma, \cos\theta\right)$ and setting $\alpha^{\parallel/\perp}$ is [5]

$$p\left(\phi, p_\gamma^{\parallel/\perp}|\Sigma\right) = \frac{\left[1 \mp p_\gamma^{\parallel/\perp}\Sigma\cos\left(2\left(\alpha^\parallel - \phi\right)\right)\right]}{\frac{1}{2\pi}\int_0^{2\pi}\mathrm{d}\phi\left[1 \mp p_\gamma^{\parallel/\perp}\Sigma\cos\left(2\left(\alpha^\parallel - \phi\right)\right)\right]}. \tag{4.17}$$

This is only true for an idealized experiment with acceptance $\epsilon = \mathrm{const}\forall\phi$, so that the acceptance $\epsilon(\phi)$ has to be included in the probability for each event. As demonstrated in reference [Har17] a Fourier series truncated after the fourth order is sufficient to model any occurring function

$$\epsilon\left(\phi\right) = \sum_{k=0}^{4} a_k \sin\left(k\phi\right) + b_k\cos\left(k\phi\right),$$

where the eight detector coefficients a_k and b_k are determined from the fit. With this the measurable probability $\tilde{p}\left(\phi, p_\gamma^{\parallel/\perp}|\Sigma, a, b\right)$ is

$$\tilde{p}\left(\phi, p_\gamma^{\parallel/\perp}|\Sigma, a, b\right) \propto \left[1 \mp p_\gamma^{\parallel/\perp}\Sigma\cos\left(2\left(\alpha^\parallel - \phi\right)\right)\right]\cdot\epsilon(\phi) \tag{4.18}$$

$$= \left[1 \mp p_\gamma^{\parallel/\perp}\Sigma\cos\left(2\left(\alpha^\parallel - \phi\right)\right)\right]\cdot\left(\sum_{k=0}^{4} a_k\sin\left(k\phi\right) + b_k\cos\left(k\phi\right)\right), \tag{4.19}$$

where $a := \{a_k\}_{k=0}^4, b := \{b_k\}_{k=0}^4$.Finally, normalizing $\frac{1}{2\pi}\int_0^{2\pi}\mathrm{d}\phi\tilde{p}\left(\phi, p_\gamma^{\parallel/\perp}|\Sigma, a, b\right) \overset{!}{=} 1$,

$$\tilde{p}\left(\phi, p_\gamma^{\parallel/\perp}|\Sigma, a, b\right) = \frac{\left[1 \mp p_\gamma^{\parallel/\perp}\Sigma\cos\left(2\left(\alpha^\parallel - \phi\right)\right)\right]\cdot\left(\sum_{k=0}^{4} a_k\sin\left(k\phi\right) + b_k\cos\left(k\phi\right)\right)}{1 \pm \frac{1}{2}a_2 p_\gamma^{\parallel/\perp}\Sigma}. \tag{4.20}$$

[5] Note: Normalizing $p\left(\phi, p_\gamma^{\parallel/\perp}|\Sigma\right)$ to 2π (or any other arbitrary constant) is sufficient for the fit as long as the integral does not depend on the fit parameters. The normalization to 2π is chosen for better readability. However, to calculate actual probabilities, one must multiply Eq. (4.17) by 2π.

The respective polarization setting $\alpha^{\parallel/\perp}$ determines the sign in the normalizing constant which allows an uncorrelated estimation of the detector coefficient a_2 and the beam asymmetry Σ. To simplify notation and implementation, Equation (4.21) can be written as *one* probability for all events – irregardless of polarization setting – if the polarization values $p_\gamma^\parallel$ are multiplied by (-1) and summarized as p_γ:

$$\tilde{p}\left(\phi, p_\gamma \middle| \Sigma, a, b\right) = \frac{\left[1 + p_\gamma \Sigma \cos\left(2\left(\alpha - \phi\right)\right)\right] \cdot \left(\sum_{k=0}^{4} a_k \sin\left(k\phi\right) + b_k \cos\left(k\phi\right)\right)}{1 - \frac{1}{2} a_2 p_\gamma \Sigma}, \tag{4.21}$$

with $\alpha = -45^\circ$ fixed.

In section 3.2 the subtraction of uncorrelated time background was discussed via a sideband subtraction. Naturally, without binning the data, this strategy is invalid and prompt peak and sideband events have to be fitted simultaneously. Hereby it is important to consider that the random time background is realized as flat distribution underneath the complete reaction time spectrum (cf. Figure 3.3), *including* the range of the prompt peak. The fraction of true coincident events to random coincidences is given as

$$f = \frac{N_{\text{prompt}} - w \cdot N_{\text{sideband}}}{N_{\text{prompt}}}, \tag{4.22}$$

where N_{prompt} and N_{sideband} are the number of events where the reaction time lies within the prompt peak or sideband, respectively. w is the ratio of the widths of the chosen prompt peak and sideband ranges, see section 3.2. It is now assumed that the random coincidences will exhibit an asymmetry Σ^{bkg} of their own and are not necessarily described by the detector coefficients a and b but rather by a^{bkg} and b^{bkg}. The probability to detect a prompt peak event p_{prompt} and the probability to measure a sideband event p_{sideband} are then given by

$$p_{\text{prompt}}\left(\phi, p_\gamma, \middle| \Sigma, a, b, \Sigma^{\text{bkg}}, a^{\text{bkg}}, b^{\text{bkg}}\right) = f \cdot \tilde{p}\left(\phi, p_\gamma \middle| \Sigma, a, b\right) + (1 - f) \cdot \tilde{p}\left(\phi, p_\gamma \middle| \Sigma^{\text{bkg}}, a^{\text{bkg}}, b^{\text{bkg}}\right) \tag{4.23}$$

$$p_{\text{sideband}}\left(\phi, p_\gamma \middle| \Sigma^{\text{bkg}}, a^{\text{bkg}}, b^{\text{bkg}}\right) = \tilde{p}\left(\phi, p_\gamma \middle| \Sigma^{\text{bkg}}, a^{\text{bkg}}, b^{\text{bkg}}\right). \tag{4.24}$$

If there are n prompt peak and m sideband events, the joint likelihood of all events $\mathcal{L}$ is thus given by

$$\mathcal{L} = \prod_{i=1}^{n} p_{\text{prompt}}\left(\phi_i, p_{\gamma,i} \middle| \Sigma, a, b, \Sigma^{\text{bkg}}, a^{\text{bkg}}, b^{\text{bkg}}\right) \prod_{j=1}^{m} p_{\text{sideband}}\left(\phi_j, p_{\gamma,j} \middle| \Sigma, a, b, \Sigma^{\text{bkg}}, a^{\text{bkg}}, b^{\text{bkg}}\right), \tag{4.25}$$

or, equivalently

$$\begin{aligned} \ln \mathcal{L} = &\sum_{i=1}^{n} \ln p_{\text{prompt}}\left(\phi_i, p_{\gamma,i} \middle| \Sigma, a, b, \Sigma^{\text{bkg}}, a^{\text{bkg}}, b^{\text{bkg}}\right) \\ &+ \sum_{j=1}^{m} \ln p_{\text{sideband}}\left(\phi_j, p_{\gamma,j} \middle| \Sigma, a, b, \Sigma^{\text{bkg}}, a^{\text{bkg}}, b^{\text{bkg}}\right). \end{aligned} \tag{4.26}$$

Eighteen[6] parameters have to be determined in total, either via a conventional frequentist approach or a Bayesian approach to this non-linear fitting problem.

Frequentist

Best fit estimates can be derived by maximizing the likelihood $\mathcal{L}$, or, for computational convenience, by minimizing $-\ln\mathcal{L}$. The *ROOT* library [BR97] offers the method *TTree::UnbinnedFit* to perform an unbinned maximum likelihood fit on data filled in a *TTree* [ROOb], which was used to perform the fit. Minimization and statistical error calculation are performed by *MINUIT* [JR75]. Errors are hereby estimated either symmetrical from the paraboloid shape of $(-\ln\mathcal{L})$ using the *HESSE* algorithm or asymmetric from the half-maximum values of $(-\ln\mathcal{L})$ using the *MINOS* algorithm without making assumptions on the shape of the likelihood, if necessary [JR75].

Bayesian

The joint posterior of all fit parameters given the data ϕ, p_γ is

$$p\left(\Sigma, a, b, \Sigma^{\mathrm{bkg}}, a^{\mathrm{bkg}}, b^{\mathrm{bkg}} \middle| \phi, p_\gamma\right) \propto \mathcal{L}\left(\phi, p_\gamma \middle| \Sigma, a, b, \Sigma^{\mathrm{bkg}}, a^{\mathrm{bkg}}, b^{\mathrm{bkg}}\right) \cdot \pi\left(\Sigma, a, b, \Sigma^{\mathrm{bkg}}, a^{\mathrm{bkg}}, b^{\mathrm{bkg}}\right), \tag{4.27}$$

where $\pi(\boldsymbol{\theta})$ denotes the combined prior of all fit parameters which factors into each individual prior since all parameters are independent:

$$\pi\left(\Sigma, a, b, \Sigma^{\mathrm{bkg}}, a^{\mathrm{bkg}}, b^{\mathrm{bkg}}\right) = \pi(\Sigma) \cdot \pi(a) \cdot \pi(b) \cdot \pi\left(\Sigma^{\mathrm{bkg}}\right) \cdot \pi\left(a^{\mathrm{bkg}}\right) \cdot \pi\left(b^{\mathrm{bkg}}\right). \tag{4.28}$$

The priors for $\Xi \in \{\Sigma, \Sigma^{\mathrm{bkg}}\}$ and $\xi \in \{a, b, a^{\mathrm{bkg}}, b^{\mathrm{bkg}}\}$ are again chosen non-informative, broadly centered around 0

$$\Xi \sim \mathcal{N}(0,1)_{[-1,1]} \qquad\qquad \xi_k \sim \mathcal{N}(0, 0.1). \tag{4.29}$$

This model, consisting of the likelihood in Eq. (4.26) and the priors in Eq. (4.29), is implemented in Stan [Sta22], so that samples from the posterior in the physically allowed region ($\Xi \in [-1,1]$) are again obtained via NUTS [HG14]. From references [Afz19; Har17] it is expected that $\xi_k \ll 1$, therefore the chosen widths of the priors resemble a, relatively speaking, broad distribution.

4.1.3 Comparison of Bayesian and frequentist approaches

The effort of implementing the binned or unbinned fit in a Bayesian approach is comparable to the traditionally used frequentist methods. Due to the probabilistic structure of the Stan language [Sta22] implementation of likelihood and prior models is straightforward and the sampling algorithms can be accessed or modified to ones needs intuitively. However, the Bayesian fit requires more careful preparation and also diagnostics. On one hand, the choice of priors has to be made. On the other hand, the fitting procedure is inherently different; not only the goodness of fit (compared with data) has to be checked but also the convergence of the Markov chains themselves. Yet, the additional effort is rewarded by the fact that the Bayesian fit will yield *distributions* for all parameters as opposed to

[6] The Fourier series is constructed such that $a_0 = 0, b_0 = 1$

point estimates with error bars. This is especially useful for polarization observables which may be used as input for PWA calculations. Here error estimates can be derived from the distributions e.g. as (multiple) standard deviations, the full width at half maximum or similar. If furthermore a Bayesian approach is pursued, also the whole distributions may be used. Another advantage of the Bayesian fit is the ability to truncate the posterior samples to the relevant or allowed parameter space.

4.2 Determination of Σ_η using Bayesian statistics

This section will now demonstrate the application of the discussed methods to obtain the beam asymmetry Σ for η photoproduction with selected data provided from reference [Afz19]. For each method only the respective Bayesian approach will be used and compared to the results from [Afz19] to confirm the that it is a valid method. As an additional sanity check toy Monte Carlo samples are generated and analyzed.

4.2.1 Application of methods to toy Monte Carlo data

Although results can be compared to the already accomplished ones in reference [Afz19], verifying the correct functioning of the fitting methods is still useful. This is done by generating events that follow the expected distributions with fixed and known parameters. These are then again fitted using the binned and unbinned fit, respectively. Repeating this for a large number of times should reproduce the input parameters if the methods work as intended.

Event yield asymmetries

The asymmetry $A(\phi)$ is built from the event yields $N^{\parallel/\perp}$, which are distributed according to

$$N^{\parallel} = N_0 \left[1 - p_\gamma^{\parallel} \Sigma \cos\left(2\left(\alpha^{\parallel} - \phi\right)\right)\right], \tag{4.30}$$

$$N^{\perp} = N_0 \left[1 - p_\gamma^{\perp} \Sigma \cos\left(2\left(\alpha^{\perp} - \phi\right)\right)\right], \tag{4.31}$$

where the parameters are chosen as $\Sigma = 0.5$, $p_\gamma^{\parallel} = 0.25$, $p_\gamma^{\perp} = 0.3$. In total, 10000 toy Monte Carlo bins are generated. In each bin the number of generated samples per setting $N_{\text{total}}^{\parallel/\perp}$ is given by a Poisson distribution

$$N_{\text{total}}^{\parallel} \sim \mathcal{P}(800) \qquad\qquad N_{\text{total}}^{\perp} \sim \mathcal{P}(1000), \tag{4.32}$$

to simulate the statistics of the $\gamma p \to p\eta$ final state as accurately as possible [Afz19]. The samples from the distributions (4.30),(4.31) are drawn using the *TH1::GetRandom* [ROOc] function provided by *ROOT* [BR97]. The function from which samples should be drawn is integrated discretely and then normalized. The normalized integral is approximated by a parabola for each bin. A random number between 0 and 1 is generated and assigned to the according bin, where the respective parabola is evaluated to give the desired random value. [ROOc].

Figure 4.2: The asymmetry $A(\phi)$ for several toy MC bins. A Bayesian fit was performed, shown here are the posterior predictive checks in comparison with a traditional χ^2 fit

Figure 4.3: Left: Combined posterior distributions of all 10000 fits normalized by their respective standard deviation (std) Right: Unaltered combined posterior distributions of all 10000 fits

Figure 4.4: Left: Monte Carlo standard error σ_{MCSE} Right: relative error $\frac{\sigma_{\mathrm{MCSE}}}{\mathrm{median}[p(\Sigma|y)]}$

Event based fit

4.2.2 Application of methods to data

Event yield asymmetries

Event based fit

4.3 Determination of $\Sigma_{\eta'}$

placeholder

4.3.1 Application of event based fit to toy Monte Carlo data

placeholder

4.3.2 Application of event based fit to data

placeholder

4.3.3 Systematic Error

placeholder

CHAPTER 5

Summary and outlook

Bibliography

[San+11] A. M. Sandorfi, S. Hoblit, H. Kamano and T.-S. H. Lee, *Determining pseudoscalar meson photoproduction amplitudes from complete experiments*, Journal of Physics G: Nuclear and Particle Physics **38** (2011) 053001, ISSN: 1361-6471, URL: http://dx.doi.org/10.1088/0954-3899/38/5/053001 (cit. on p. 33).

[Afz19] F. N. Afzal, *Measurement of the beam and helicity asymmetries in the reactions $\gamma p \to p\pi^0$ and $\gamma p \to p\eta$*, PhD thesis: Rheinische Friedrich-Wilhelms-Universität Bonn, 2019, URL: https://hdl.handle.net/20.500.11811/8064 (cit. on pp. 34, 35, 39, 40).

[Afz+20] F. Afzal et al., *Observation of the $p\eta'$ Cusp in the New Precise Beam Asymmetry Σ Data for $\gamma p \to p\eta$*, Phys. Rev. Lett. **125** (15 2020) 152002, URL: https://link.aps.org/doi/10.1103/PhysRevLett.125.152002 (cit. on p. 34).

[RP22] G. van Rossum and the Python development team, *The Python Language Reference, Release 3.10.5*, 2022, URL: https://docs.python.org/3.10/reference/index.html (cit. on p. 36).

[Vir+20] P. Virtanen et al., *SciPy 1.0: Fundamental Algorithms for Scientific Computing in Python*, Nature Methods **17** (2020) 261 (cit. on p. 36).

[BR97] R. Brun and F. Rademakers, *ROOT — An object oriented data analysis framework*, Nucl. Instrum. Meth. A **389** (1997) 81, ISSN: 0168-9002, URL: https://www.sciencedirect.com/science/article/pii/S016890029700048X (cit. on pp. 36, 39, 40).

[sci] scipy, *scipy.optimize.curve_fit, Function Documentation*, URL: https://docs.scipy.org/doc/scipy/reference/generated/scipy.optimize.curve_fit.html (visited on 28/06/2022) (cit. on p. 36).

[ROOa] ROOT, *TH1 Class reference*, URL: https://root.cern.ch/doc/master/classTH1.html#a63eb028df86bc86c8e20c989eb23fb2a (visited on 28/06/2022) (cit. on p. 36).

[Sta22] Stan development team, *Stan Modeling Language Users Guide and Reference Manual*, vol. 2.29, 2022, URL: https://mc-stan.org (cit. on pp. 36, 39).

[HG14] M. D. Hoffman and A. Gelman, *The No-U-Turn Sampler: Adaptively Setting Path Lengths in Hamiltonian Monte Carlo*, Journal of Machine Learning Research **15** (2014) 1593, URL: http://jmlr.org/papers/v15/hoffman14a.html (cit. on pp. 36, 39).

[Har17] J. Hartmann, *Measurement of Double Polarization Observables in the Reactions $\gamma p \rightarrow p\pi^0$ and $\gamma p \rightarrow p\eta$ with the Crystal Barrel/TAPS Experiment at ELSA*, Rheinische Friedrich-Wilhelms-Universität Bonn, 2017, URL: https://hdl.handle.net/20.500.11811/7258 (cit. on pp. 37, 39).

[ROOb] ROOT, *TTree Class reference*, URL: https://root.cern.ch/doc/master/classTTree.html#a3e6bf252ab8653b47cc9116950f3ee7b (visited on 28/06/2022) (cit. on p. 39).

[JR75] F. James and M. Roos, *Minuit - a system for function minimization and analysis of the parameter errors and correlations*, Computer Physics Communications **10** (1975) 343, ISSN: 0010-4655, URL: https://www.sciencedirect.com/science/article/pii/0010465575900399 (cit. on p. 39).

[ROOc] ROOT, *TF1 Class reference*, URL: https://root.cern.ch/doc/master/classTF1.html#a410b0219e18e80d3e305b4d97374c077 (visited on 28/06/2022) (cit. on p. 40).

List of Figures

List of Tables